the fluidity of these examples probably involves primarily interactions between the particles (*12*). The lunar avalanches suggest that, irrespective of air buoyancy, avalanches can behave efficiently like fluids composed of rapidly moving particles.

The idea that masses of rock fragments can exhibit fluid behavior in the absence of liquids or gases has important implications for geologic transport mechanisms on the moon. For instance, base surges (*13*) or analogous radial flows could be produced by impact events in the absence of a gas phase. Furthermore, where geologic characteristics such as relict stratigraphy do not demand it, it may not be necessary to posit air lubrication to account for efficient avalanches on the earth.

Data from the Apollo 17 mission may make it possible to determine whether the large avalanche at the landing site originated locally and moved in the absence of gas. In any event, the characteristics of smaller lunar avalanches (Fig. 2) strongly imply that gas-free rock flows occur.

Note added in proof: Rocks collected from the Apollo 17 bright mantle are like those from the adjacent mountain to the south, which supports the avalanche interpretation (*19*). Photographic evidence obtained during the Apollo 17 mission increases the likelihood that this avalanche was triggered by secondary impacts from Tycho (*19*). The small sizes of secondary craters in the vicinity suggests that the kinetic energy added to the avalanche by these impacts is small compared to the potential energy of falling (10^{22} ergs). The plotted position of the Apollo 17 avalanche in Fig. 3, therefore, would change but little if this kinetic energy were added; the problem of the "efficiency" of this avalanche remains.

KEITH A. HOWARD
U.S. Geological Survey,
Menlo Park, California 94025

References and Notes

1. D. H. Scott, B. K. Lucchitta, M. H. Carr, "Geologic maps of the Taurus-Littrow region of the moon—Apollo 17 premission maps" [*U.S. Geol. Surv. Misc. Geol. Invest. Map I-800* (1972)].
2. E. W. Wolfe, V. L. Freeman, W. R. Muehlberger, J. W. Head, H. H. Schmitt, J. R. Sevier, *Geotimes* **17** (No. 11), 14 (1972).
3. R. L. Shreve, *Science* **154**, 1639 (1966).
4. ———, *Geol. Soc. Amer. Spec. Pap. 108* (1968).
5. M. R. Mudge, *Geol. Soc. Amer. Bull.* **76**, 1003 (1965).
6. Another type of apparent lunar debris flow is represented by a much larger and thicker lobate avalanche which extends radially outward from the crater Tsiolkovsky. This lobe may have been mobilized by impact fluids, and its radial orientation suggests that the driving force included the cratering event as well as gravity.
7. P. E. Kent, *J. Geol.* **74**, 79 (1966); R. L. Shreve, *Geol. Soc Amer. Bull.* **79**, 653 (1968). Dry snow avalanches behave as density currents of mixed air and particles [M. Mellor, *U.S. Army Cold Regions Res. Eng. Lab. Monogr.* (part 3, sect. A3) (1968), p. 17], and the fluid behavior of some rock avalanches has been similarly attributed [see (*8*, *11*)].
8. D. R. Crandell and R. K. Fahnestock, *U.S. Geol. Surv. Bull. 1221-A* (1965).
9. This assumes a specific gravity of 2 (so that the weight of the deposit on the moon is 6.5×10^{16} dynes), an average height of fall of 1700 m, and distances of 1900 m (vertical) and 9000 m (horizontal) from the top of the denuded zone to the distal end.
10. S. Sekiya and Y. Kikuchi, *J. Coll. Sci. Imp. Univ. Tokyo* **3** (part 2), 91 (1889).
11. D. J. Varnes, *Nat. Res. Counc. Highw. Res. Board Spec. Rep. 29* (1958), p. 20.
12. R. A. Bagnold [*Proc. Roy. Soc. Ser. A Math. Phys. Sci.* **225**, 49 (1954)] suggests a theoretical approach for particle flow in which inertial effects dominate over fluid-viscosity effects.
13. G. A. Young, *The Physics of the Base Surge* (U.S. Naval Ordnance Laboratory, White Oak, Md., 1965).
14. A. S. Post, *Nat. Acad. Sci. Publ. 1603* (1968), p. 266; *U.S. Geol. Surv. Prof. Pap. 544-D* (1967). I have assumed average thicknesses of 3 m for the Allen, Fairweather, and Schwan 1 avalanches, 5 m for the Schwan 2 avalanche, 2 m for the Sioux avalanche, and 1.3 m for the Steller avalanche.
15. J. V. Harrison and N. L. Falcon, *J. Geol.* **45**, 296 (1938).
16. K. Howard, unpublished data, Galápagos Islands.
17. J. B. Hadley, *U.S. Geol. Surv. Prof. Pap. 435-K* (1964), p. 107.
18. M. C. Hoyer, *Geol. Soc. Amer. Bull.* **82**, 1267 (1971).
19. W. R. Muehlberger *et al.*, in *Apollo 17 Preliminary Science Report* (National Aeronautics and Space Administration, Washington, D.C., in press).
20. I thank G. Plafker, E. W. Wolfe, and H. H. Schmitt for discussions and helpful suggestions. Supported by NASA contract W13,130 and experiment S-222. Publication authorized by the director, U.S. Geological Survey.

7 December 1972; revised 9 February 1973

■

Monoclinic Hydroxyapatite

Abstract. *The existence of a monoclinic phase of hydroxyapatite, $Ca_5(PO_4)_3OH$, has been confirmed, by single-crystal structure analysis (weighted "reliability" factor = 3.9 percent on $|F|^2$). The structure has space group* $P2_1/b$, *a = 9.4214(8) angstroms,* b = 2a, *c = 6.8814(7) angstroms, and* $\gamma = 120°$, *and is analogous to that of chlorapatite. The distortions from the hexagonal structure with which the monoclinic structure is pseudosymmetric are similar to those in chlorapatite, including enlargement of that triangular array of oxygen atoms in which the chlorine ion or, in hydroxyapatite, the hydroxyl hydrogen ion is approximately centered. The hydroxyapatite specimen was prepared by the conversion of a single crystal of chlorapatite in steam at 1200°C, was mimetically twinned, and was approximately 37 percent monoclinic.*

The agriculturally and scientifically important apatite minerals, their technologically (lighting, catalysis, laser host) important synthetic counterparts, and the closely related "mineral" portion of bones and teeth have, until recently, been thought to occur only with hexagonal crystal symmetry in crystallographic space group $P6_3/m$. A monoclinic pseudohexagonal form, space group $P2_1/b$, of both synthetic (*1*, *2*) and mineral (*3*) forms of chlorapatite has recently been reported for specimens with nearly stoichiometric (for example, less than 5 to 15 percent deficient) chlorine contents. In both forms the chlorine ions occur in columns. In the monoclinic form they are fully ordered within columns and the columns are ordered relative to each other (*1*, *4*). In the hexagonal form the lack of full intracolumn ordering is statistically representable as twofold disorder of the chlorine positions about mirror planes which, in the monoclinic form, become glide planes.

In hexagonal hydroxyapatite the hydroxyl ions are similarly arranged in columns in twofold disorder with the O → H direction pointing away from the mirror planes passing through the nearest coordinating calcium ions (*5*). It was recognized (*5*) that adjacent hydroxyl ions in a given column must occur in a head-to-tail fashion, that is, O–H O–H O–H, otherwise the H–H approach would be too close. It was later shown (*6*) that the fluorine impurities in the mineral (from Holly Springs, Georgia) were distributed and that they provided reversal points for the sense of the O–H direction within a column. It was then conjectured [see, for example, Young (*7*) and Elliott (*8*)] that a hydroxyapatite specimen, sufficiently free of impurities and vacanies so that no significant number of such reversal points were present within the column, might also exhibit intercolumn ordering and, hence, the monoclinic $P2_1/b$ space group, analogously to chlorapatite. Elliott reported (*9*) that the diffraction pattern of hydroxyapatite crystals prepared from essentially stoichiometric chlorapatite single crystals, heated in steam at 1200°C for 2 weeks (*10*), exhibited "extra" reflections explicable on the basis of the $P2_1/b$ space group for hydroxyapatite and mimetic twinning such as is commonly observed with chlorapatite having that space group.

A point of particular interest about a monoclinic form of hydroxyapatite arises from (i) its role as the model substance for the inorganic fraction of bone coupled with (ii) the reported bioelectric effect by which bone growth is influenced by electric currents or fields (*11*). Posner (*12*), among others, has noted that the very small crystallites of hydroxyapatite in bone could well be of dimension smaller than is typical for the distances between column-ordering reversal points in larger crystals and thus could be primarily composed of ordered columns with, possibly, significant intercolumn ordering, as well. Monoclinic chlorapatite has been reported (*13*) to undergo transition to a ferroelectric form under the action of a relatively weak electric field. If monoclinic hydroxyapatite were to behave similarly, the polar nature of the resulting crystal could be an important factor in the bioelectric effects in bone growth. The work presented here was undertaken in an effort to enhance or to deny the implications of both intracolumn and intercolumn ordering of hydroxyl ions and, if the ordering were confirmed, to provide enough atomic-scale detail to permit some insight into the ordering mechanism.

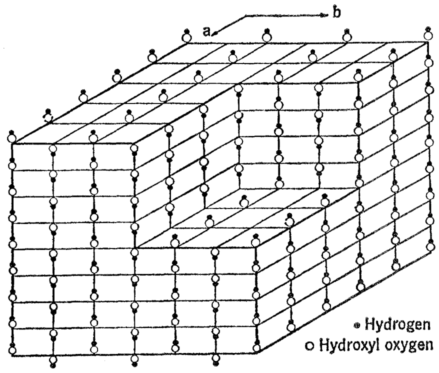

Fig. 1. Schematic representation of the ordered arrangement of hydroxyl ions in monoclinic, $P2_1/b$, hydroxyapatite. The rest of the unit cell content, consisting of calcium and phosphate ions, has been omitted for clarity.

The crystal specimen, a spheroid 0.4 mm in diameter, was prepared from a synthetic chlorapatite single crystal by essentially the same method used earlier (*10*). The apparent space group ($P2_1/b$) and twinning (*14*) were confirmed with Weissenberg photographs, and the specimen was then mounted on a computer-controlled four-circle diffractometer employing MoKα radiation ($\lambda = 0.70926$ Å). From a least-squares analysis with the instrument settings corresponding to 12 reflections, the lattice parameters and the standard deviations in them were determined to be $a = 9.4214(8)$ Å and $c = 6.8814(7)$ Å with the constraints $b = 2a$ and $\gamma = 120°$. Refinements without these constraints led to $a = b/2$ within 8×10^{-3} Å and $\gamma = 120°$ within 5′.

The lattice parameters of chlorapatite (*4*) are $a = 9.628(5)$ Å and $c = 6.764(5)$ Å, and those of synthetic hydroxyapatite (*1*) are $a = 9.422(3)$ Å and $c = 6.883(3)$ Å. Thence, by Vegard's law, within an experimental uncertainty of approximately 2 percent, the crystal specimen for this work was pure hydroxyapatite, free of chlorine.

The intensities of 1944 independent reflections were measured (*15*). Of these, 892 were "monoclinic reflections," that is, do not occur for the hexagonal structure to which the actual, monoclinic structure is pseudosymmetric. These reflections, for which k is odd and $\ell \neq 0$, are not superimposed by the twinning, as are those for which k is even. All 892 k-odd reflections were from only one of the three "crystals" in the twin. Measurements of k-odd reflections permitted an estimate of the relative fraction (0.31, 0.32, 0.37) of the specimen associated with each of the three crystal positions in the twin.

Least-squares refinements of the monoclinic structure were carried out with all 1944 reflections on the assumption that, because of the strong hexagonal pseudosymmetry, the relative intensities among the triply superimposed "hexagonal" reflections (k-even) were the same as they would be for an untwinned specimen (*16*). Because the reflections for k-odd and those for k-even had been collected in different experiments, they were assigned different (adjustable) scale factors in the least-squares refinements. The structure parameters for hexagonal Holly Springs hydroxyapatite (*17*) were taken for

Table 1. Crystal structure parameters obtained for monoclinic hydroxyapatite. (All parameters except those for site occupancy have been multiplied by 10^4. Standard deviations are shown in parentheses.)

Atom	Site-occupancy factor	Refined coordinates			Anisotropic temperature factors					
		x	y	z	β_{11}	β_{22}	β_{33}	β_{12}	β_{13}	β_{23}
$\mathrm{O_{IA}}$	1.008(8)	3286(3)	4918(2)	2604(5)	34(3)	7(1)	31(4)	11(2)	− 1(5)	0(2)
$\mathrm{O_{IB}}$	1.018(7)	4850(2)	3282(1)	7604(5)	22(3)	3(1)	36(3)	3(2)	1(4)	6(2)
$\mathrm{O_{IC}}$	1.013(7)	1568(2)	5858(1)	2462(5)	11(2)	10(1)	48(3)	8(2)	− 1(6)	0(3)
$\mathrm{O_{IIA}}$	1.024(8)	5866(3)	4828(2)	2365(5)	16(3)	8(1)	74(5)	4(2)	14(4)	1(2)
$\mathrm{O_{IIB}}$	1.036(6)	5359(2)	3105(1)	2422(5)	26(3)	5(1)	89(4)	13(2)	−10(5)	5(3)
$\mathrm{O_{IIC}}$	1.032(7)	1213(3)	5438(1)	7319(4)	32(3)	6(1)	53(5)	2(2)	6(4)	6(2)
$\mathrm{O_{IIIA}}$*	1.016(10)	3280(4)	3746(2)	821(4)	44(5)	9(1)	34(4)	18(3)	−11(4)	−11(2)
$\mathrm{O_{IIIB}}$	1.003(10)	7473(4)	2904(2)	804(4)	35(5)	11(1)	42(4)	−2(3)	23(4)	− 8(2)
$\mathrm{O_{IIIC}}$*	1.009(8)	794(3)	4134(2)	5817(3)	37(4)	14(1)	30(3)	24(3)	−13(3)	− 2(2)
$\mathrm{O'_{IIIA}}$*	1.025(8)	3578(3)	3827(1)	4404(3)	25(3)	8(1)	28(3)	13(2)	0(2)	5(1)
$\mathrm{O'_{IIIB}}$	1.020(10)	7373(4)	2949(2)	4390(4)	40(5)	8(1)	33(4)	4(3)	−15(4)	2(2)
$\mathrm{O'_{IIIC}}$	1.033(10)	909(4)	4290(2)	9397(4)	26(4)	7(10)	29(4)	11(2)	2(3)	− 2(2)
$\mathrm{Ca_{I}}$	0.998(3)	3259(1)	5798(1)	6(1)	18(1)	5(0)	20(1)	2(1)	− 1(1)	− 1(0)
$\mathrm{Ca'_{I}}$	0.989(3)	3412(1)	5868(1)	4977(1)	18(1)	6(0)	21(1)	3(1)	2(1)	0(0)
$\mathrm{Ca_{IIA}}$	0.995(2)	2465(1)	2465(0)	2534(1)	22(1)	5(0)	32(1)	4(0)	− 2(2)	1(1)
$\mathrm{Ca_{IIB}}$	0.995(3)	−68(1)	6233(0)	7434(1)	19(1)	6(0)	23(1)	6(0)	− 5(1)	1(1)
$\mathrm{Ca_{IIC}}$	0.983(3)	2533(1)	3732(0)	7567(1)	21(1)	6(0)	24(1)	6(0)	3(1)	− 1(1)
$\mathrm{P_{A}}$	1.030(4)	3982(1)	4342(0)	2556(2)	17(1)	4(0)	22(1)	6(1)	− 3(2)	0(1)
$\mathrm{P_{B}}$	1.033(4)	6315(1)	2650(0)	2552(2)	16(1)	4(0)	25(1)	2(1)	− 3(2)	1(1)
$\mathrm{P_{C}}$	1.027(3)	302(1)	4490(0)	7518(2)	14(1)	5(0)	27(1)	5(1)	1(2)	− 1(1)
$\mathrm{O_{H}}$	1.012(10)	− 7(3)	2504(2)	3045(3)	31(4)	6(1)	82(4)	10(3)	− 2(3)	1(2)
H	1.000	0	2500	4392	129	32	104	32	0	0

* The temperature factors of these atoms are nonpositive definite (see text).

the starting points. Absorption corrections were made with tabulated data (*18*) for spheres [$\mu r = 0.58$ (μ is the absorption coefficient and r is the radius)]. Using the correction formula of Zachariasen (*19*), we made extinction corrections iteratively with the least-squares refinement cycles in separate passes.

Observations of the intensities of 28 k-odd reflections at both room temperature and ~50°C verified that the monoclinic structure also exists at body temperature (that is, 37°C).

The final cycle of least-squares refinement of the structural model yielded wR_2, the weighted "reliability" factor based on $|F|^2$, equal to 3.9 percent and the structural parameters given in Table 1. Although certain anomalies in the temperature factors remain (those for O_{IIIA}, O_{IIIC}, and O'_{IIIA} are nonpositive definite, possibly because of the assumption discussed in footnote (*16*) or the fact, commented on below, that only part of the specimen was monoclinic), the structure refinement has successfully proceeded far enough to confirm the monoclinic structural form and to permit discussion of its main features. The positions of the hydrogen atoms have been deduced from the positions (in twofold disorder) found in the neutron diffraction studies of Holly Springs hydroxyapatite (*5*). The monoclinic cell is related to the usual one used for hexagonal apatites by a translation of b(hex)/2 as well as by doubling of one of the hexagonal axes (b). The notation for the atoms follows that used for hexagonal apatite structures with additional designations to allow for atoms that are not symmetry-related in the monoclinic structure although they are in the hexagonal structure.

The most interesting feature of the monoclinic hydroxyapatite structure, and that which had been expected by analogy with monoclinic chlorapatite, is the ordered arrangement of the hydroxyl ions. This is illustrated in Fig. 1. There is a close similarity between the distortions from hexagonal symmetry found in this structure and those found in monoclinic chlorapatite (*4*), including the (unforeseen) fact that the O_{III} triangle which is enlarged by having a chlorine ion near its center in chlorapatite is also the one which contains the hydroxyl hydrogen in hydroxyapatite.

Not all of the specimen was in the monoclinic phase. Analysis of the separately refined scale factors for the "monoclinic" (k-odd) reflections and the hexagonal (k-even) reflections led to the conclusion that the specimen was approximately 63 percent hexagonal and 37 percent monoclinic. Preliminary data for another crystal suggest that this ratio may vary greatly from specimen to specimen and may, therefore, be a point of interest for future studies.

This confirmation of the existence of a monoclinic phase of hydroxyapatite has potential significance in several fields. For example, interest is heightened in exploration of the dielectric properties of the monoclinic phase both in terms of fundamental solid-state properties (probably analogous to those of monoclinic chlorapatite) and in terms of possible involvement in bioelectric effects on bone growth. The existence of monoclinic hydroxyapatite also removes a previously apparent inconsistency between the morphological symmetry (tape-like) of developing dental enamel crystals and their crystal symmetry, which was previously thought to be constrained to hexagonal but is now recognized to have the possibility of being monoclinic.

J. C. ELLIOTT
Georgia Institute of Technology,
Atlanta, Georgia 30332, and
London Hospital Medical College,
London, England

P. E. MACKIE
R. A. YOUNG
Georgia Institute of Technology

References and Notes

1. R. A. Young and J. C. Elliott, *Arch. Oral Biol.* **11**, 699 (1966).
2. J. S. Prener, *J. Electrochem. Soc.* **114**, 77 (1967).
3. A. W. Hounslow and G. Y. Chao, *Can. Mineral.* **10**, 252 (1970).
4. P. E. Mackie, J. C. Elliott, R. A. Young, *Acta Cryst. Sect. B* **28**, 1840 (1972).
5. M. I. Kay, R. A. Young, A. S. Posner, *Nature* **204**, 1050 (1964).
6. R. A. Young, W. van der Lugt, J. C. Elliott, *ibid.* **223**, 729 (1969).
7. R. A. Young, *Trans. N.Y. Acad. Sci.* **29**, 949 (1967).
8. J. C. Elliott, *Calcif. Tissue Res.* **3**, 293 (1969).
9. ———, *Nature* **230**, 72 (1971).
10. ——— and R. A. Young, *ibid.* **214**, 904 (1967).
11. C. A. L. Bassett, R. J. Pawluk, R. O. Becker, *ibid.* **204**, 652 (1964).
12. A. S. Posner, *Physiol. Rev.* **49**, 760 (1969).
13. J. C. Elliott and R. A. Young, *Bull. Soc. Chim. France* (**n° special**), 1763 (1968).
14. Three distinct crystal positions occur in the twin, related by 120° rotations about the c axis; none of the more than ten specimens so produced was free of twinning.
15. Details of the technique, which employed both Zr-filtered and unfiltered radiation, have been described elsewhere [see (*4*); P. E. Mackie, thesis, Georgia Institute of Technology (1972)].
16. Although this assumption was satisfactory for the present purpose of confirming the existence of monoclinic hydroxypatite, it clearly does not hold in principle and will have to be abandoned in more detailed refinements of the monoclinic structure. Some confidence in its acceptability here is imparted by the fact that the final wR_2 based on the k-even reflections alone was 4.0 percent, whereas that for the k-odd reflections was 13.9 percent.
17. K. Sudarsanan and R. A. Young, *Acta Cryst. Sect. B* **25**, 1534 (1969).
18. C. H. MacGillavry and G. D. Rieck, Eds., *International Tables for X-Ray Crystallography* (Kynoch, Birmingham, England, 1962), vol. 3.
19. W. H. Zachariasen, *Acta Cryst.* **16**, 1139 (1963).
20. This work has received financial support from the U.S. Public Health Service through National Institute of Dental Research grant DE 01912 and from the United Kingdom Science Research Council.

6 October 1972; revised 15 February 1973

Ice Nucleation: Elemental Identification of Particles in Snow Crystals

Abstract. *A scanning field-emission electron microscope combined with an x-ray analyzer is used to locate the ice nucleus within a three-dimensional image of a snow crystal and determine the chemical composition of the nucleus. This makes it possible to better understand the effect of nuclei in cloud seeding.*

Information about the elemental composition of atmospheric nuclei is necessary for a quantitative evaluation of deliberate and inadvertent weather modification. In seeding experiments on supercooled clouds, AgI is most often used as the seeding agent. Because the presence of silver in seeded snow can be due to nucleation, scavenging, or sedimentation, analyzing the silver concentration in the snow provides information about the spatial and temporal distribution of AgI in a particular seeding area. However, this method provides little information about the effectiveness of the seeding agent in any weather modification attempt. Only by examining individual AgI particles in relation to individual snow crystals and identifying AgI as the nucleus is it possible to make an objective analysis of seeding experiments.

Using the principle that a particle can act as a nucleus in its own supersaturated solution, Parungo and Rhea (*1*) developed a technique for growing AgI crystals smaller than a micrometer but large enough to be analyzed with an optical microscope and thereby identified as ice nuclei. However, this